Exact analytical results for quantum walks on star graphs

2009 J. Phys. A: Math. Theor. 42 115205

(http://iopscience.iop.org/1751-8121/42/11/115205)

IOP PUBLISHING JOURNAL OF PHYSICS A: MATHEMATICAL AND THEORETICAL

J. Phys. A: Math. Theor. **42** (2009) 115205 (8pp) doi:10.1088/1751-8113/42/11/115205

Exact analytical results for quantum walks on star graphs

Xin-Ping Xu

Institute of Particle Physics, HuaZhong Normal University, Wuhan 430079, People's Republic of China
and
Institute of High Energy Physics, Chinese Academy of Science, Beijing 100049, People's Republic of China

Received 27 November 2008, in final form 3 February 2009
Published 20 February 2009
Online at stacks.iop.org/JPhysA/42/115205

Abstract

In this paper, we study coherent exciton transport of continuous-time quantum walks on star graphs. Exact analytical results of the transition probabilities are obtained by means of the Gram–Schmidt orthonormalization of the eigenstates. Our results show that the coherent exciton transport displays perfect revivals and strong localization on the initial node. When the initial excitation starts at the central node, the transport on a star graph is equivalent to the transport on a complete graph of the same size.

PACS numbers: 05.60.Gg, 05.60.Cd, 71.35.−y

(Some figures in this article are in colour only in the electronic version)

The problem of coherent and non-coherent transport modeled by random walks has attracted much attention in many distinct fields, ranging from polymer physics to biological physics, from solid-state physics to quantum computation [1–4]. The random walk is related to diffusion models and is a fundamental topic in discussions of Markov processes. Several properties of random walks, including dispersal distributions, first-passage times and encounter rates, have been extensively studied [5, 6]. As a natural extension to the quantum world of ubiquitous classical random walks, quantum walks (QWs) have also been introduced and widely investigated in the literature [7].

An important application of quantum walks is that they can be used to design highly efficient quantum algorithms. For example, Grover's algorithm can be combined with quantum walks in a quantum algorithm for glued trees which provides an exponential speed up over classical methods [8, 9]. Besides their important applications in quantum algorithms, quantum walks are also used to model the coherent exciton transport in solid-state physics [10]. It is shown that the dramatic nonclassical behavior of quantum walks can be attributed to quantum coherence, which does not exist in classical random walks.

There are two main types of quantum walk: continuous-time and discrete-time quantum walks. The main difference between them is that discrete-time walks require a coin which is just any unitary matrix plus an extra Hilbert space on which the coin acts, while continuous-time walks do not need this extra Hilbert space [11]. Apart from this difference, the two types of quantum walks are analogous to continuous-time and discrete-time random walks in the classical case [11]. Discrete-time quantum walks evolve by the application of a unitary evolution operator at discrete-time intervals, and continuous-time quantum walks evolve under a time-independent Hamiltonian. Unlike the classical case, the discrete-time and continuous-time quantum walks cannot be simply related to each other by taking a limit as the time step goes to zero [12]. Both types of quantum walk have been defined and studied on discrete structures in the market.

Here, we focus on continuous-time quantum walks (CTQWs). Most previous studies related to CTQWs in the last decade concentrate on regular structures such as lattices, and most of the common wisdom concerning them relies on the results obtained in this particular geometry. Exact analytical results for CTQWs are also found for some particular regular structures, such as the cycle graph [13] and Cayley tree [14]. Exact analytical results are difficult to get due to the cumbersome analytical investigations of the eigenvalues and eigenstates of the Hamiltonian.

In this paper, we consider CTQWs on star graphs, and get exact analytical results for the first time. The star graph is one of the most regular structures in graph theory and represents the local tree structure of irregular and complex graphs. In mathematical language, a star graph of size N consists of one central node and $N-1$ leaf nodes. All the leaf nodes connect to the central node, and there is no connection between the leaf nodes. Therefore, the central node has $N-1$ bonds and the leaf nodes have only one bond. As we will show, for such simple topology, we are able to derive exact analytical results for the transition probabilities. These analytical results exactly agree with the numerical results obtained by diagonalizing the Hamiltonian H using the software MATLAB.

The coherent exciton transport on a connected network is modeled by the continuous-time quantum walks (CTQWs), which are obtained by replacing the Hamiltonian of the system by the classical transfer matrix, i.e., $H = -T$ [15, 16]. The transfer matrix T relates to the Laplace matrix by $T = -A$. The Laplace matrix A has nondiagonal elements A_{ij} equal to -1 if nodes i and j are connected and 0 otherwise. The diagonal elements A_{ii} are equal to degree of node i, i.e., $A_{ii} = k_i$. The states $|j\rangle$ endowed with the node j of the network form a complete, ortho-normalized basis set, which spans the whole accessible Hilbert space. The time evolution of a state $|j\rangle$ starting at time t_0 is given by $|j,t\rangle = U(t,t_0)|j\rangle$, where $U(t,t_0) = \exp[-\mathrm{i}H(t-t_0)]$ is the quantum-mechanical time evolution operator. The transition amplitude $\alpha_{k,j}(t)$ from state $|j\rangle$ at time 0 to state $|k\rangle$ at time t reads $\alpha_{k,j}(t) = \langle k|U(t,0)|j\rangle$ and obeys the Schrödinger equation [17]. Then the classical and quantum transition probabilities to go from state $|j\rangle$ at time 0 to state $|k\rangle$ at time t are given by $p_{k,j}(t) = \langle k|\,\mathrm{e}^{-tA}|j\rangle$ and $\pi_{k,j}(t) = |\alpha_{k,j}(t)|^2 = |\langle k|\,\mathrm{e}^{-\mathrm{i}tH}|j\rangle|^2$ [18], respectively. Using E_n and $|q_n\rangle$ to represent the nth eigenvalue and ortho-normalized eigenvector of H, the classical and quantum transition probabilities between two nodes can be written as [17, 18]

$$p_{k,j}(t) = \sum_n \mathrm{e}^{-tE_n}\langle k|q_n\rangle\langle q_n|j\rangle, \tag{1}$$

$$\pi_{k,j}(t) = |\alpha_{k,j}(t)|^2 = \left|\sum_n \mathrm{e}^{-\mathrm{i}tE_n}\langle k|q_n\rangle\langle q_n|j\rangle\right|^2. \tag{2}$$

For finite networks, the classical transition probabilities approach the equal-partition $1/N$. However, quantum transport does not lead to equal-partition. $\pi_{k,j}(t)$ does not decay *ad infinitum* but at some time fluctuates about a constant value. This value is determined by the long time average of $\pi_{k,j}(t)$ [17, 18],

$$\begin{aligned}\chi_{k,j} &= \lim_{T\to\infty}\frac{1}{T}\int_0^T \pi_{k,j}(t)\,\mathrm{d}t \\ &= \sum_{n,l}\langle k|q_n\rangle\langle q_n|j\rangle\langle j|q_l\rangle\langle q_l|k\rangle \\ &\quad\times \lim_{T\to\infty}\frac{1}{T}\int_0^T \mathrm{e}^{-\mathrm{i}t(E_n-E_l)}\,\mathrm{d}t \\ &= \sum_{n,l}\delta_{E_n,E_l}\langle k|q_n\rangle\langle q_n|j\rangle\langle j|q_l\rangle\langle q_l|k\rangle. \end{aligned} \tag{3}$$

where δ_{E_n,E_l} takes value 1 if E_n equals E_l and 0 otherwise. In order to calculate $p_{k,j}(t)$, $\pi_{k,j}(t)$ and $\chi_{k,j}$, all the eigenvalues E_n and eigenstates $|q_n\rangle$ are required. For the star graph, in the following, we will first analytically calculate the eigenvalues and eigenstates, then give exact analytical results for the transition probabilities according to the above equations.

For a specific star graph of size N, we label the central node as node 1 while the leaf nodes are numbered as $2, 3, \ldots, N$. Because of the centrosymmetric structure of the star graph, there are only four types of transition probabilities, namely, $\pi_{1,1}(t)$, $\pi_{2,1}(t) \equiv \pi_{1,2}(t)$, $\pi_{2,2}(t)$ and $\pi_{3,2}(t) \equiv \pi_{2,3}(t)$. Transition probabilities between other nodes belong to these four types. Therefore, we only consider the four kinds of probabilities listed above. The Hamiltonian of the star graph can be written as

$$H = (N-1)|1\rangle\langle 1| + \sum_{i=2}^{N}(|i\rangle\langle i| - |1\rangle\langle i| - |i\rangle\langle 1|). \tag{4}$$

The eigenvalues of the Hamiltonian have three discrete values: $E_1 = E_2 = \cdots = E_{N-2} = 1$, $E_{N-1} = 0$ and $E_N = N$ [19]. One set of eigenstates $\{|v_i\rangle\}$ $(i = 1, 2, \ldots, N)$ corresponding to the eigenvalues is $|v_i\rangle = |i+2\rangle - |2\rangle$ $(i = 1, 2, \ldots, N-2)$, $|v_{N-1}\rangle = \sum_{i=1}^{N}|i\rangle$ and $|v_N\rangle = \sum_{i=1}^{N}|i\rangle - N|1\rangle$. However, this set of eigenstates is not orthogonal ($\langle v_1|v_2\rangle \neq 0$, etc); we use the Gram–Schmidt process [20] to orthogonalize this set of eigenstates. The Gram–Schmidt algorithm is a method for orthogonalizing a set of vectors in an inner product space [21], and the new orthogonal vectors $\{|v_i'\rangle\}(i = 1, 2, \ldots, N-2)$ are given by the following formula:

$$|v_i'\rangle = |v_i\rangle - \sum_{j=1}^{i-1}\frac{\langle v_i|v_j'\rangle}{\langle v_j'|v_j'\rangle}|v_j'\rangle, \tag{5}$$

where $|v_1'\rangle = |v_1\rangle$ is applied in the iterative process [20, 21]. According to the above equation, we obtain

$$|v_i'\rangle = \begin{cases} |i+2\rangle - \dfrac{1}{i}\displaystyle\sum_{j=2}^{i+1}|j\rangle, & i = 1, 2, \ldots, N-2 \\ |v_i\rangle, & i = N-1, N. \end{cases} \tag{6}$$

The above new eigenstates $\{v_i'\rangle\}$ are not normalized (i.e., $\langle v_i'|v_i'\rangle \neq 1$, etc). After some algebraic calculations, we get the orthonormal basis $\{|q_i\rangle\}$ as follows:

$$|q_i\rangle = \begin{cases} \sqrt{\dfrac{i}{i+1}}|i+2\rangle - \sqrt{\dfrac{1}{i(i+1)}}\displaystyle\sum_{j=2}^{i+1}|j\rangle, & i = 1, 2, \ldots, N-2 \\ \sqrt{1/N}\displaystyle\sum_{j=1}^{N}|j\rangle, & i = N-1 \\ \dfrac{1}{\sqrt{N(N-1)}}\displaystyle\sum_{i=1}^{N}|i\rangle - \sqrt{\dfrac{N}{N-1}}|1\rangle, & i = N. \end{cases} \tag{7}$$

One can easily prove that $\{|q_i\rangle\}$ is also a set of eigenstates of the Hamiltonian (i.e., $H|q_i\rangle = E_i|q_i\rangle, \forall\, i$). $\{|q_i\rangle\}$ forms an orthonormal and complete basis satisfying $\langle q_i|q_j\rangle = \delta_{ij}$ and $\sum_j |q_j\rangle\langle q_j| = 1$. Therefore, we can use this set of eigenstates $\{|q_i\rangle\}$ to calculate the transition probabilities in equations (1), (2) and (3).

Substituting the orthonormal basis of equation (7) into equation (2), we get $\pi_{1,1}(t)$ and $\pi_{2,1}(t)$ as follows:

$$\pi_{1,1}(t) = \frac{N^2 - 2N + 2}{N^2} + \frac{2(N-1)}{N^2}\cos Nt. \tag{8}$$

$$\pi_{2,1}(t) = \frac{2}{N^2} - \frac{2}{N^2}\cos Nt. \tag{9}$$

For $\pi_{2,2}(t)$ and $\pi_{3,2}(t)$, the calculation is analogous, but the expressions are cumbersome:

$$\begin{aligned}\pi_{2,2}(t) = \frac{1}{N^2(N-1)^2}[&(N^4 - 4N^3 + 5N^2 - 2N + 2) + (2N^3 - 6N^2 + 4N)\cos t \\ &+ (2N^2 - 4N)\cos(N-1)t + (2N-2)\cos Nt],\end{aligned} \tag{10}$$

$$\begin{aligned}\pi_{3,2}(t) = \frac{2}{N^2(N-1)^2}[&(N^2 - N + 1) + (N - N^2)\cos t - N\cos(N-1)t \\ &+ (N-1)\cos Nt].\end{aligned} \tag{11}$$

Other transition probabilities can also calculated, but they have the same expressions as equations (8)–(11). For instance, $\pi_{4,2}(t)$ has the same analytical form as $\pi_{3,2}$, which is consistent with our intuition. Analogously, we can get the long time averages of the transition probabilities

$$\begin{aligned}\chi_{1,1} &= (N^2 - 2N + 2)/N^2 \\ \chi_{2,1} &= 2/N^2 \\ \chi_{2,2} &= (N^4 - 4N^3 + 5N^2 - 2N + 2)/N^2/(N-1)^2 \\ \chi_{3,2} &= 2(N^2 - N + 1)/N^2/(N-1)^2.\end{aligned} \tag{12}$$

The transition probabilities depend on the size of the graph. In the thermodynamic limit of the infinite network $N \to \infty$, the transport displays high localizations on the initial position, i.e., $\chi_{i,j} \approx \delta_{i,j}$. In contrast, for the classical transport modeled by continuous-time random walks, the transition probabilities do not show any oscillation and approach the equal-partition $1/N$ at long times [19]. According to equation (1), the four-type transition probabilities can be written as

$$\begin{aligned}p_{1,1}(t) &= 1/N + \mathrm{e}^{-Nt}(N-1)/N \\ p_{2,1}(t) &= 1/N - \mathrm{e}^{-Nt}/N \\ p_{2,2}(t) &= 1/N + (N-2)/(N-1)\,\mathrm{e}^{-t} + \mathrm{e}^{-Nt}/N/(N-1) \\ p_{3,2}(t) &= 1/N - \mathrm{e}^{-t}/(N-1) + \mathrm{e}^{-Nt}/N/(N-1).\end{aligned} \tag{13}$$

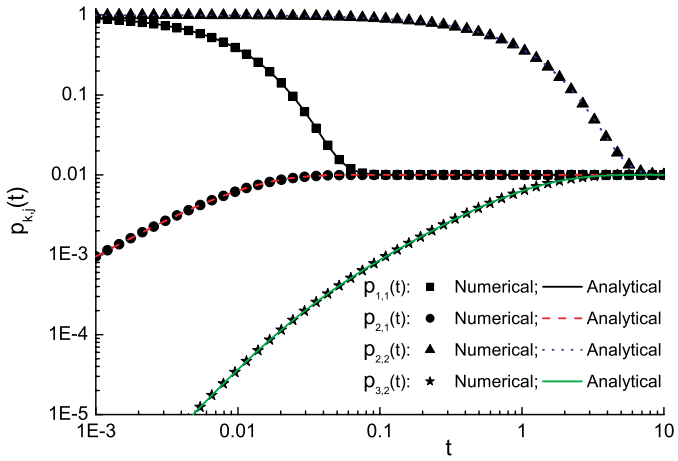

Figure 1. Classical transition probabilities $p_{k,j}(t)$ versus t. The marked points are numerical results and the curves are analytical predictions in equation (13).

In order to test the analytical predictions, we compare the classical $p_{k,j}(t)$ predicted by equation (13) with the numerical results obtained by numerically diagonalizing the Hamiltonian. The results for a star graph of $N = 100$ are shown in figure 1. As we can see, the numerical results exactly agree with the analytical prediction in equation (13). The transport reaches the equal-partitioned distribution $1/N$ at long times. However, when the excitation starts at the central node, the transport reaches the equal partition more quickly than the transport which starts at the leaf nodes (compare the curves in figure 1).

For the quantum transport, we compare the transition probabilities in figure 2. The numerical results (marked as black squares) exactly agree with the theoretical results in equations (8)–(11). We note that all the transition probabilities show periodic recurrences. Comparing $\pi_{1,1}(t)$ and $\pi_{2,2}(t)$ (see figure 2(*a*) and (*c*)), we find that there are high probabilities of finding the exciton at the initial node. This suggests that the coherent transport shows high localizations on the initial nodes [19]. The oscillation amplitudes of the return probabilities $\pi_{1,1}(t)$ and $\pi_{2,2}(t)$ are comparable but the oscillation periods are quite different. The oscillating period of $\pi_{2,2}(t)$ is 100 (N) times of that of $\pi_{1,1}(t)$. This could be interpreted by the analytical expressions in equations (8) and (10). Similar behavior also holds for $\pi_{2,1}(t)$ and $\pi_{3,2}(t)$ (see figure 2(*b*) and (*d*)), but the oscillation amplitude is smaller than the return probabilities. This also can be understood from the analytical results in equations (9) and (11), where the transition probability is mainly determined by the high order term of N. The small value of the oscillating period of $\pi_{2,1}(t)$ and $\pi_{1,1}(t)$ suggests that there are frequent revivals when the exciton starts at the central node, compared to the transport starting at the leaf nodes.

The quantum limiting probabilities in equation (12) are only a function of the graph size N. Figure 3 shows the quantum limiting probabilities for numerical results and theoretical predictions. Both the results agree with each other. We find that the return probabilities $\chi_{1,1}$ and $\chi_{2,2}$ are an incremental function of N and approach 1 in the limit $N \to \infty$. In contrast, $\chi_{2,1}$ and $\chi_{3,2}$ decrease with N and close to $2/N^2$ in the limit $N \to \infty$. We note that $\chi_{1,1}$ differs from $\chi_{2,2}$ for small values of N. Such deviation diminishes as N increases. This suggests that the strength of localizations is almost the same for central-node and leaf-node excitations. The only difference is that the frequency of revivals (oscillation period) for central-node excitation is much higher than that for leaf-node excitation.

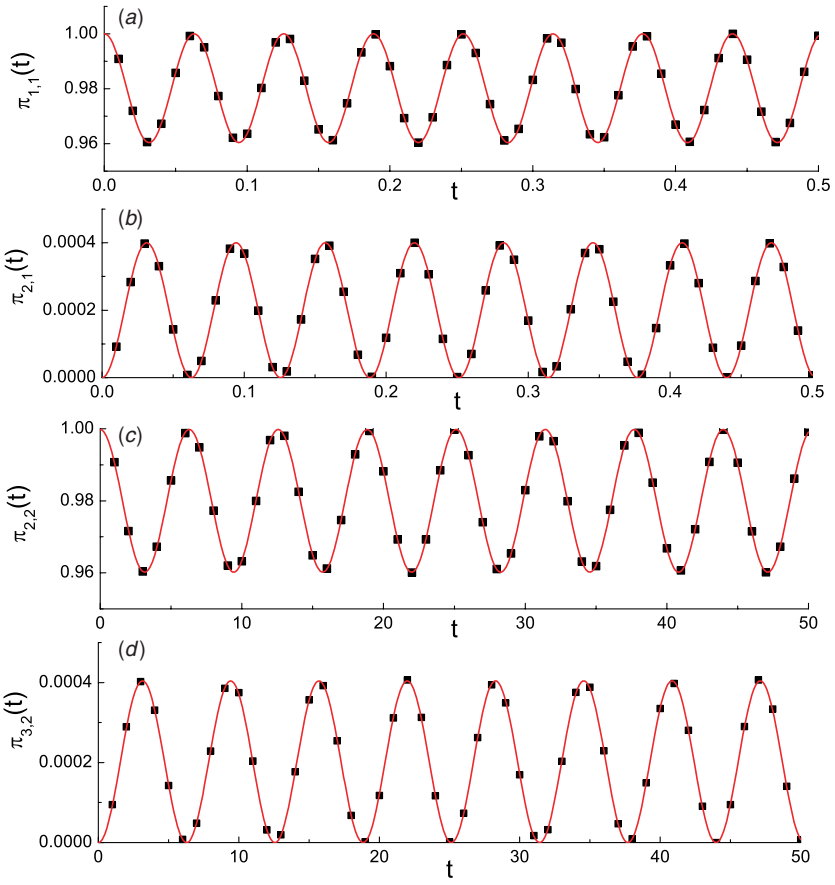

Figure 2. Quantum transition probabilities $\pi_{1,1}(t)$ (*a*), $\pi_{2,1}(t)$ (*b*), $\pi_{2,2}(t)$ (*c*) and $\pi_{3,2}(t)$ (*d*). The points denoted by black squares are numerical results and the curves are theoretical predictions in equations (8)–(11).

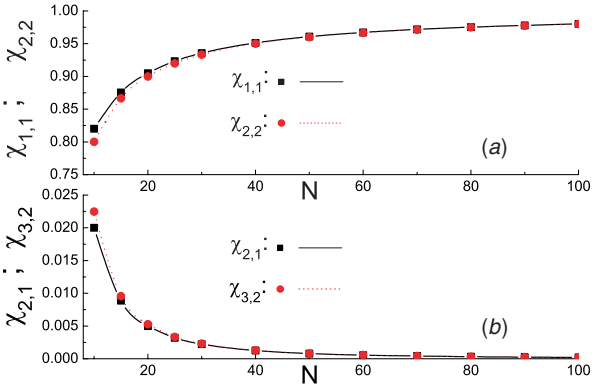

Figure 3. Long-time limiting probabilities $\chi_{1,1}$, $\chi_{2,2}$ (*a*) and $\chi_{2,1}$, $\chi_{3,2}$ (*b*) as a function of the network size *N*. The points marked as symbols are numerical results and the curves are analytical results predicted by equation (12).

To address the similarities and differences between the star graph and the complete graph, we proceed to consider the transport on a complete graph of size N. The complete graph is fully connected, thus the Hamiltonian is given by $H = (N-1)\sum_i |i\rangle\langle i| - \sum_{i\neq j} |i\rangle\langle j|$. The eigenvalues are two different values: $E_1 = E_2 = \cdots = E_{N-1} = N$ and $E_N = 0$. One set of non-orthogonal states $\{|v_i\rangle\}$ corresponding to the eigenvalues can be written as $|v_i\rangle = |i+1\rangle - |1\rangle$ $(i = 1, 2, \ldots, N-1)$ and $|v_N\rangle = \sum_{j=1}^{N} |j\rangle$. Using the Gram–Schmidt orthonormalization (see equation (5)), the orthonormal basis for a complete graph is

$$|q_i\rangle = \begin{cases} \sqrt{\dfrac{i}{i+1}}|i+1\rangle - \sqrt{\dfrac{1}{i(i+1)}}\displaystyle\sum_{j=1}^{i}|j\rangle, & i = 1, 2, \ldots, N-1 \\ \sqrt{1/N}\displaystyle\sum_{j=1}^{N}|j\rangle, & i = N. \end{cases} \tag{14}$$

Substituting the above equation into equation (2), we get the quantum transition probabilities for the complete graph

$$\pi_{i,j}(t) = \begin{cases} \dfrac{N^2-2N+2}{N^2} + \dfrac{2(N-1)}{N^2}\cos Nt, & i = j \\ \dfrac{2}{N^2} - \dfrac{2}{N^2}\cos Nt. & i \neq j. \end{cases} \tag{15}$$

We note that equation (15) has exactly the same form as equations (8) and (9). This indicates that the transport starting at the central node on a star graph is equivalent to the transport on a complete graph of the same size.

In summary, we have studied coherent exciton transport of continuous-time quantum walks on star graphs. Exact analytical results of the transition probabilities are obtained in terms of the Gram–Schmidt orthonormalization. We find that the coherent transport shows perfect recurrences and there is a high frequency of revivals for central-node excitation. Study of long time averages suggests that the quantum transport displays strong localizations on the initial node. When the initial excitation starts at the central node, the transport on a star graph is equivalent to the transport on a complete graph of the same size.

Acknowledgments

This work is supported by the National Natural Science Foundation of China under projects 10575042, 10775058 and MOE of China under contract number IRT0624 (CCNU). We thank Professor Blumen (University of Freiburg) for useful discussions.

References

[1] Guillotin-Plantard N and Schott R 2006 *Dynamic Random Walks: Theory and Application* (Amsterdam: Elsevier)
[2] Woess W 2000 *Random Walks on Infinite Graphs and Groups* (Cambridge: Cambridge University Press)
[3] Supriyo D 2005 *Quantum Transport: Atom to Transistor* (London: Cambridge University Press)
[4] Mello P A and Kumar N 2004 *Quantum Transport in Mesoscopic Systems: Complexity and Statistical Fluctuations* (Oxford: Oxford University Press)
[5] Metzler R and Klafter J 2000 *Phys. Rep.* **339** 1
[6] Burioni R and Cassi D 2005 *J. Phys. A: Math. Gen.* **38** R45
[7] Farhi E and Gutmann S 1998 *Phys. Rev.* A **58** 915
[8] Grover L K 1996 A fast quantum mechanical algorithm for database search *Proc. 28th Annual ACM Symposium on Theory of Computing* (New York: ACM) pp 212–9
[9] Yin Y, Katsanos D E and Evangelou S N 2008 *Phys. Rev.* A **77** 022302

[10] Kittel C 1986 *Introduction to Solid State Physics* (New York: Wiley)
[11] Krovi H and Brun T A 2007 *Phys. Rev.* A **75** 062332
[12] Strauch F W 2006 *Phys. Rev.* A **74** 030301
[13] Solenov D and Fedichkin L 2003 *Phys. Rev.* A **73** 012313
[14] Mülken O and Blumen A 2005 *Phys. Rev.* E **71** 016101
[15] Mülken O and Blumen A 2005 *Phys. Rev.* E **71** 036128
[16] Xu X P, Li W and Liu F 2008 *Phys. Rev.* E **78** 052103
[17] Volta A, Mülken O and Blumen A 2006 *J. Phys. A: Math. Gen.* **39** 14997
[18] Xu X P 2008 *Phys. Rev.* E **77** 061127
[19] Mülken O and Blumen A 2006 *Phys. Rev.* E **73** 066117
[20] http://www.math.hmc.edu/calculus/tutorials/gramschmidt/
[21] Arfken G 1985 *Mathematical Methods for Physicists* 3rd edn (Orlando: Academic) pp 516–20